4-Pixel Heterodyne Receiver at 1.9 THz using a CMOS Spectrometer

Jenna L. Kloosterman[1,*], Jonathan H. Kawamura[1], Adrian J. Tang[1,2], Rod Kim[2], Jose Siles[1], Fahouzi Boussaha[3], Bruce Bumble[1], Choonsup Lee[1], Alejandro Peralta[1], Robert Lin[1], Imran Mehdi[1]
[1]*Jet Propulsion Laboratory, California Institute of Technology, 91106 Pasadena, CA, USA*
[2]*University of California, Los Angeles, Los Angeles, CA 90095, USA*
[3]*Observatoire de Paris, 75014 Paris, France*
*Contact: Jenna.L.Kloosterman@jpl.nasa.gov

Abstract— This paper reports on engineering results from a high-sensitivity 4x1-pixel 1.9 THz heterodyne array for the astrophysically important [CII] spectral line. A 4-pixel multiplier chain at 1.9 THz, with a compact spacing of 5 mm, is used as an LO. Superconducting Hot Electron Bolometers (HEB) are used as mixers. Receiver performance is verified by y-factor measurements with measured sensitivities of 900 K uncorrected. Spectral measurements were obtained by mixing a coherent source near the target frequency of 1.9 THz and down converting the IF to baseband. Spectra were recorded with both an IBOB and a newly available CMOS-based spectrometer for comparison. This paper is the first to report on spectra obtained by CMOS spectrometer technology and this spectrometer provides several advantages over more traditional FFT spectrometers because of its compact size and low power consumption. This 4x1 receiver prototype is easily scalable to other frequencies and larger focal plane arrays. Furthermore, because of its compact configuration, it can be easily packaged for orbital or sub-orbital missions.

I. Introduction

Large spectroscopic THz arrays are needed for surveys that can resolve large-scale motions within giant molecular clouds (GMCs) to formulate a more complete understanding of the star formation process and the lifecycle of the Interstellar Medium (ISM). Because of atmospheric attenuation, most important atomic and molecular species are only visible from near space or space, the most important being 1.9 THz (158 μm) fine structure line of [CII]. The *Herschel Space Observatory* [1], launched in 2009, carried the first 1.9 THz heterodyne receiver as part of the Heterodyne Instrument for the Far Infrared (HIFI) [2]. The list of receivers at 1.9 THz that have flown since HIFI is short. The German Receiver for Astronomy at Terahertz Frequencies (GREAT) [3-4] followed by upGREAT [5-6] have operated in flight on the Stratospheric Observatory for Infrared Astronomy (SOFIA) [7]. upGREAT contains two 7-pixel arrays, one for each polarization. The Stratospheric Terahertz Observatory (STO) [8] and the Stratospheric Terahertz Observatory – 2 (STO-2) [9] contained multiple 1.9 THz pixels and the Galactic/Extragalactic ULDB (ultra-long duration balloon) Stratospheric Terahertz Observatory (GUSTO) was just selected under the NASA Explorer's Program for a launch in 2021.

Airborne and balloon flights provide for comparatively large mass and power margins. For the next generation of THz heterodyne arrays to be appealing to a broader range of platforms such as a CubeSat or a satellite, receivers with more compact configurations and lower power consumption are needed. This paper presents lab measurements from a compact 4-pixel array receiver. Heterodyne performance is verified with simultaneous measurements of spectra using a second 1.9 THz source and an IBOB spectrometer. Finally, measurements from the first use of a CMOS-based spectrometer are presented.

II. Instrument Description

A. Local Oscillator

The LO is a frequency multiplied source with 4 individual pixels spaced 5 mm apart. The compact design is only 18 x 10 x 12 cm and uses around 24 W of power. The multiplier chain, shown in Figure 1, uses a QuickSyn synthesizer to drive the AMC. The signal is then amplified by a GaN power amplifier and split 4 ways. Each pixel has its own set of Schottky diode triplers chained together to output power at 220 GHz, 650, GHz and 1.9 THz. Furthermore, each of these triplers can be biased individually to maximize power output for each pixel. Measured powers for each pixel on the LOat 1.9 THz were in the 20-40 μW range. This also provides a mechanism to tune each pixel individually, which is necessary to optimize pump power for each HEB mixer.

B. Optics

For lab testing we used two 30 deg off axis parabolic mirrors with a focal length of ~100 mm. The first mirror focused the LO power and signal through the center of the window. The second mirror, attached to the cold plate inside the cryostat, redirected the LO power and signal to the mixer block via a folding mirror. These optics were a cheaper alternative than machining a larger cryostat window to couple LO from all 4 pixels simultaneously.

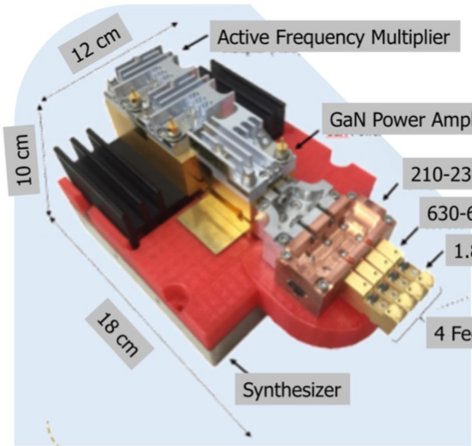

Figure 1. Compact 4-pixel 1.9 THz frequency multiplier chain.

C. HEB Mixer Module

The 4-pixel HEB mixer block uses a matching diagonal feed horn array to that of the LO. The pixel spacing for each is only 5 mm. The compact mixer block measures 30 x 10 x 10 mm when assembled as seen in Figure 2. The front half contains diagonal feed horns and a very short 1.9 THz waveguide. To machine diagonal feed horns, an E-plane split through the middle of the block is necessary. The back half contains a pocket for the mixer chip and feed thrus to GPO connectors for IF signals.

The mixers are made from silicon-on-insulator (SOI) chip technology. The HEB sits in the center of a bowtie antenna on the chip. The SOI chips are then inserted and subsequently wirebonded into a 2 mm x 2 mm backshell constructed from photolithograpy and micro-plating techniques. The backshells ensure that the mixer is precisely aligned to the front piece of the mixer block 1.9 THz waveguide. A ground connection between the mixer block and the HEB device is made when the backshell contacts the front feed horn array [10].

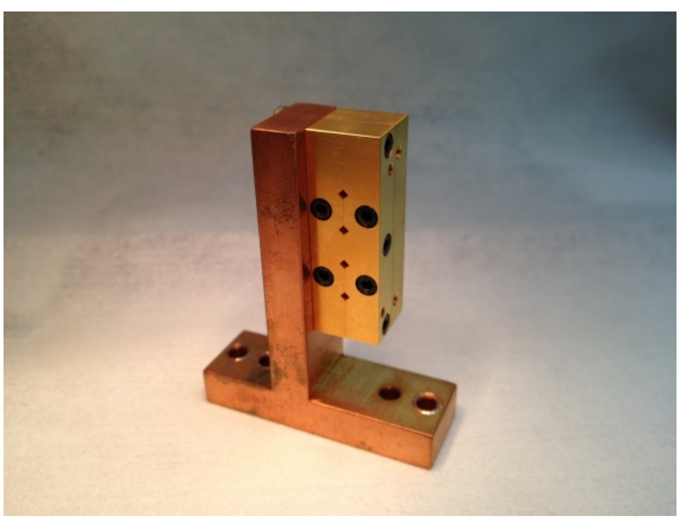

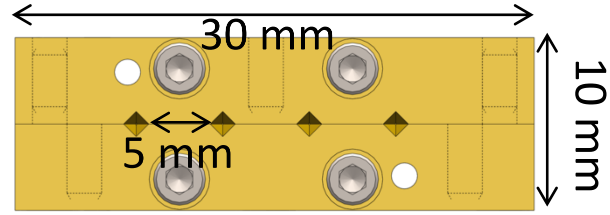

Figure 2. Photograph (below) and model (above) of a compact 4-pixel HEB mixer block.

The optics, mixer bock, and LNAs for all 4 pixels can been seen installed inside the cryostat in Figure 3. The cryostat was originally designed for one pixel and has been subsequently retrofitted for two and then four pixel systems.

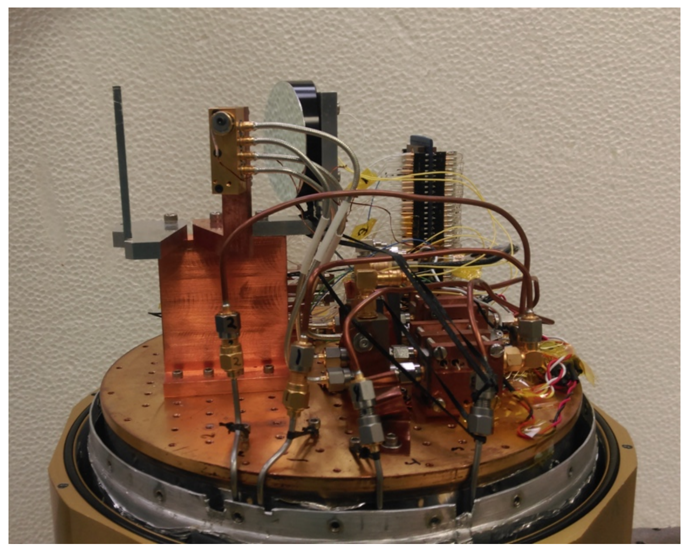

Figure 3. 4-pixel HEB system installed inside the cryostat.

D. IF Electronics

A bias-tee is attached to the IF output of every pixel and the bias circuitry is contained inside the cryostat, controlled by a bias box and NI-DAQ on the outside. The IF LNAs are clamped to the 4 K cold plate. Outside of the cryostat, the receiver is completed by room temperature amplifiers and filters. For y-factor measurements the IF is readout by an Agilent power meter. For spectral measurements, the IF goes through a second down conversion to baseband.

E. Spectrometers

This paper demonstrates the receiver's functionality using two different spectrometers, a more traditional FPGA IBOB spectrometer and a new CMOS-based spectrometer. The CMOS-based spectrometer uses a UCLA-JPL developed system-on-chip (SOC) technology containing the digitizers, FFT processors, and USB readout circuitry to provide highly integrated low-power spectral processing. The entire SOC is about the size of a credit card and draws an order of magnitude less power over its FPGA predecessor. This spectrometer design is described in more detail in Ref. [11].

III. Measurements And Results

A. Receiver Performance

Initial optical alignment was completed by shining a laser through the optics before the cryostat was closed and cooled. The window was removed during the laser alignment. The LO was mounted to a 3-axis stage. This setup is very similar to the one shown in Figure 6, although y-factor measurements did not use the 1.9 THz source, only the 4-pixel LO. Once cold the HEB currents were monitored until all 4 pixels were maximally pumped at the same time. I-V curves taken simultaneously were recorded with a LabView program and replotted in Figure 4. Room temperature resistances and critical currents from unpumped I-V curves (not shown) are summarized in TABLE 1.

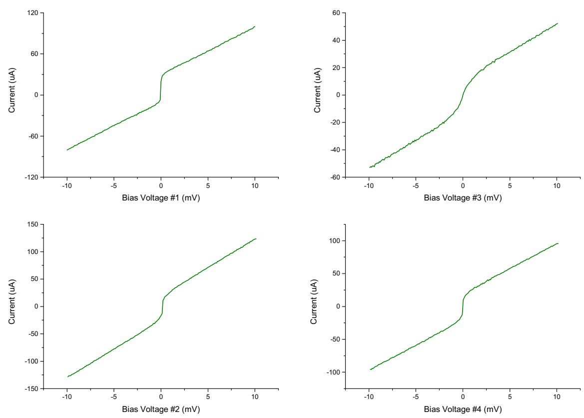

Figure 4. The 4-pixel LO is simultaneously pumping all 4 HEB mixers.

Each pixel was then measured for sensitivity using the y-factor method. A wire grid was used to inject warm and cold blackbody loads into the cryostat while sweeping the HEB in bias voltage. The measurements and calculated DSB noise temperature measurements are shown in Figure 5. The warm load at 290 K, is shown in red, and the liquid nitrogen load, 80 K, is shown in blue. The resulting DSB noise temperature is shown in black. The two best pixels were pixels 1 and 4 with double sideband noise temperatures of ~900 K uncorrected. Pixels 2 and 3 had devices that were slightly below and above the target room temperature resistance of 100 Ω, respectively. This creates an impedance mismatch with the IF circuity when cold thus degrading the overall performance of the mixer.

TABLE 1. ROOM TEMPERATURE AND COLD TEMPERATURE RESISTANCES, CRITICAL CURRENTS, AND NOISE TEMPERATURES FOR ALL 4 PIXELS.

Pixel	Ω_{RT}	Ω_{100K}	I_C (μA)	$T_{RX,DSB}$ (K)
1	109	126	130	900
2	82	93	165	1800
3	130	179	30	1700
4	105	120	185	900

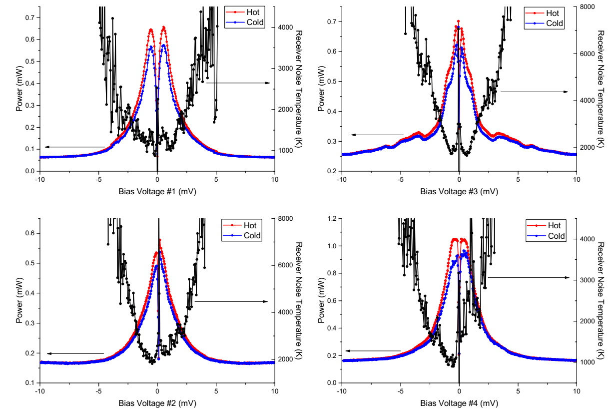

Figure 5. Sensitivity measurements for 4-pixel HEB array. The warm load (290 K) is in red. The cold load (80 K) is in blue. The calculated noise temperature is in black.

B. Spectral Measurements

1. IBOB Spectrometer: After verifying the performance of the receiver, a tone at 1.8977976 THz was quasi-optically injected via the polarizer grid and observed at baseband by all 4 pixels simultaneously with IBOB spectrometers. A picture of the setup can be seen in Figure 6 and the results of the LSB measurements can be seen in Figure 7. The tone moved through the band pass when it was adjusted in frequency. To illustrate this observation, a second frequency is shown at 1.8978300 THz, which is ~34 MHz from the initial tone. The measurements have been normalized to 1.

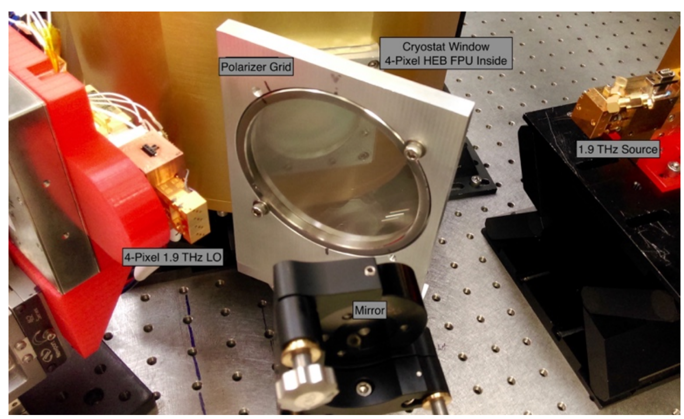

Figure 6. Measurement setup for spectral measurements at 1.9 THz.

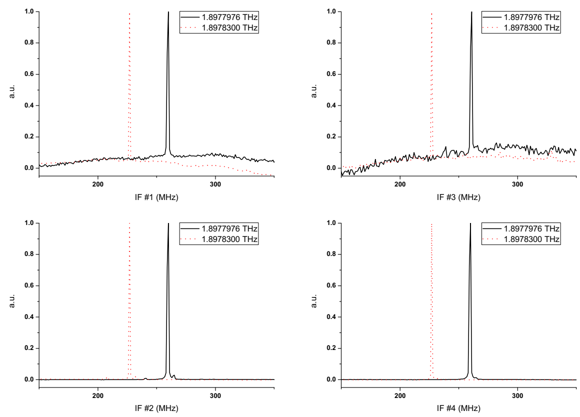

Figure 7. Spectral measurements using an IBOB spectrometer for two different tones near 1.9 THz. The measurements from each tone were taken simultaneously and only the LSB is shown. Tones have been normalized to 1.

2. CMOS-Based 2.0 GHz Complex FFT Spectrometer: Finally, following the verification of heterodyne performance of the receiver using an IBOB spectrometer, the use of a new CMOS spectrometer was demonstrated. At the time of the 4-pixel measurements, a single 2.0 GHz Complex FFT spectrometer with 256 channels was available. The 2 GHz naming refers to the maximum possible input clock frequency, which determines the maximum spectrometer bandwidth. Power consumption for this spectrometer typically runs about 500 mW. It was designed with Earth and planetary science applications in mind, and subsequently had options for other Stokes' Parameters to compute a complex FFT. For galactic observations of [CII], only the real FFT would be used and power consumption would be lowered with the same number of channels.

The first measurement of this new spectrometer was an Allan Variance to determine stability. In order to take the measurement, noise from the receiver baseband amplifiers was injected into the spectrometer. This measurement, shown in Figure 8, was taken over a night lasting 15.5 hours. Two channels of the spectrometer were chosen at random to compute the spectroscopic Allan Variance time, which is nearly ~10,000 s. However, the error bars on this measurement grow larger as fewer data points were available for averaging.

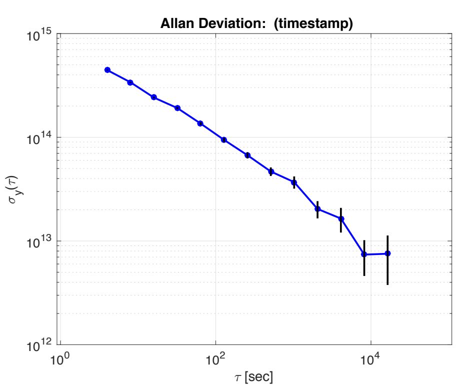

Figure 8. Allan variance measurement for the CMOS 2.0 GHz spectrometer.

Next, the spectral measurements at 1.9 THz with the receiver were repeated with this spectrometer. Due to the limitation of only one available spectrometer, one signal was recorded at a time, but the setup shown in Figure 6 did not otherwise change and the baseband configuration remained the same. The resulting spectra are shown for the LSB in Figure 9 for 1 GHz of bandwidth.

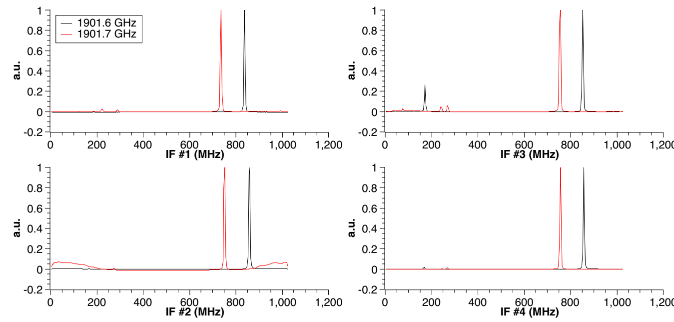

Figure 9. LSB measurements of a 1.9 THz receiver.

A final Allan Variance test was done for the end-to-end receiver using Pixel 4. For this test, the frontend of the receiver was stabilized through a PID loop between the 660 GHz tripler LO bias voltage and the HEB mixer current. Once again two spectrometer channels were chosen at random to calculate the spectroscopic Allan Variance time. Shown in Figure 10, this measurement resulted in a spectroscopic receiver Allan Time of ~5 seconds.

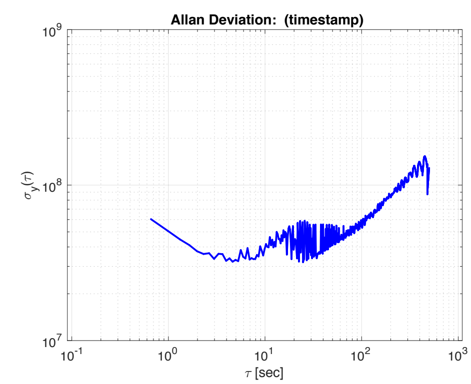

Figure 10. The stabilized end-to-end receiver spectroscopic Allan Variance for Pixel 4.

3. 2.6 GHz Real FFT Spectrometer: A newer version of the CMOS spectrometer with a maximum 2.6 GHz clock frequency became available and was tested using the 557 GHz water line. This version was designed for only real inputs and subsequently drew about the same amount of power as the previous version, despite having 4 times as many channels for a much higher spectral resolution. The measurement setup included a gas cell containing water vapor at 1 mTorr against a 77 K reference load and a 500-600 GHz room temperature Schottky receiver. The spectrometer was placed in a small red 3-D printed box. The box, shown in Figure 11, provides a scale of the size of an SOC. The spectrum recorded at 557 GHz from this setup is shown in Figure 12.

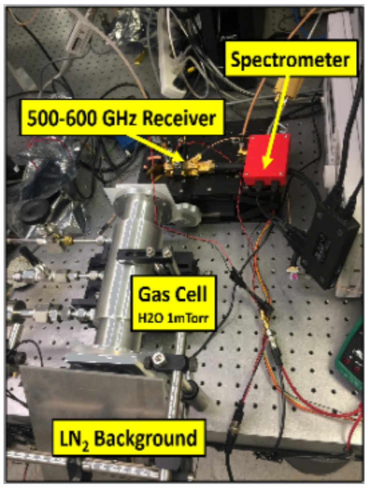

Figure 11. The measurement setup for the demonstration of a 557 GHz receiver using the new 2.6 GHz Real FFT SOC spectrometer.

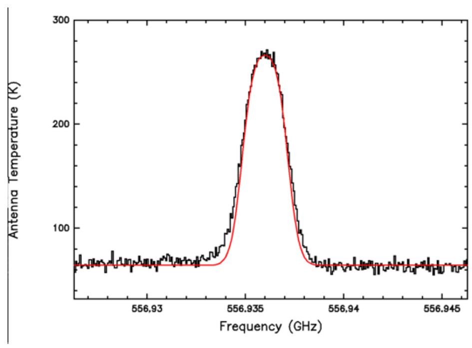

Figure 12. Spectrum of water vapor recorded at 557 GHz during a simulated 1800-second observation. The receiver, which is operated in ambient air, stares through a 25 cm column of room temperature water vapor gas held at 1 mTorr against a 77 K reference load. The red curve is the model brightness temperature from Ref. [12].

IV. Discussion

A. Lesson Learned from the Mixer Block Design

The 4-pixel mixer block used in this paper had continual problems with wire bonds from the IF signal lifting from the post of the GPO connector. This lead to a number of the better matched HEB devices breaking as the mixer block was opened and closed a number of times to re-bond the wires. It was determined that issue with the wire bonds was a result of the post of the GPO connector being too close to the HEB backshell to make a good loop. Subsequently, designs of future blocks have doubled the space left between these and should improve the mixer block assembly process.

B. Larger-Format HEB Focal Plane Arrays

After completing a 4-pixel 1.9 THz receiver, the next steps were to design and fabricate a 16-pixel LO [13] and a 16-pixel mixer block [14]. The new design not only corrects for the problem identified in Section IV-A, it also uses Picket-Potter feed horns with a circular to rectangular waveguide transition, which can be directly drilled without an E-plane split that is needed for a traditional diagonal feed horn [15]. Furthermore, these feed horns also have the added bonus of a lower cross-polarization.

B. FPGA and CMOS Spectrometer Comparison

CMOS spectrometers will have distinct advantages over the more traditional FPGA-based spectrometers, especially for space-based applications due to their compact size and lower power consumption. The IBOB used for this paper is the size of a record player and draws an average of 25-30 W. On the other hand, the new CMOS-based technology has shown it can match the spectral resolution and bandwidth of an FPGA-based FFT spectrometer at a fraction of the size and power consumption.

V. Summary and Conclusion

The 4-pixel HEB receiver has been demonstrated end-to-end using a 4-pixel LO and a 4-pixel mixer module. The 4-pixel LO draws only 24 W of power, a factor of 2 less than its 4-pixel predecessor and in a more compact configuration [16]. The receiver demonstrates high sensitivity with 2 pixels at 900 K DSB uncorrected. Finally, spectra using an FPGA-based IBOB spectrometer were compared to spectra using new CMOS technology. This new technology has demonstrated that the CMOS technology is a compact, low-powered viable alternative to the power hungry and large FPGA FFT spectrometers. With advances in frequency multiplier chains, mixer block design and fabrication, and CMOS technology, this receiver demonstrates a new compact, low-powered technology for space-based THz applications.

Acknowledgment

The research was carried out at the Jet Propulsion Laboratory, California Institute of Technology, under a contract with the National Aeronautics and Space Administration.

References

[1] G. L. Pilbratt, J. R. Riedinger, T. Passvogel, G. Crone, D. Doyle, U. Gageur, A. M. Heras et al., "Herschel Space Observatory-An ESA facility for far-infrared and submillimetre astronomy," *Astronomy & Astrophysics,* vol. 518, p. L1, July 2010.
[2] T. De Graauw, F. P. Helmich, T. G. Phillips, J. Stutzki, E. Caux, N. D. Whyborn, P. Dieleman et al., "The Herschel-heterodyne instrument for the far-infrared (HIFI)," *Astronomy & Astrophysics,* vol. 518, p. L6, July 2010.
[3] S. Heyminck, U. U. Graf, R. Güsten, Jürgen Stutzki, H. W. Hübers, and P. Hartogh, "GREAT: the SOFIA high-frequency heterodyne instrument," *Astronomy & Astrophysics,* vol. 542, p. L1, June 2012.
[4] P. Pütz, C. E. Honingh, K. Jacobs, M. Justen, M. Schultz, and J. Stutzki, "Terahertz hot electron bolometer waveguide mixers for GREAT." *Astronomy & Astrophysics* vol. 542, p. L2, June 2012.
[5] C. Risacher, R. Güsten, J. Stutzki, H-W. Hübers, A. Bell, C. Buchbender, D. Büchel et al., "The upGREAT 1.9 THz multi-pixel high resolution spectrometer for the SOFIA Observatory," *Astronomy & Astrophysics,* vol. 595, p. A34, Nov. 2016.
[6] C. Risacher *et al*., "First Supra-THz Heterodyne Array Receivers for Astronomy With the SOFIA Observatory," in *IEEE Transactions on Terahertz Science and Technology*, vol. 6, no. 2, pp. 199-211, March 2016.
[7] E. T. Young, E. E. Becklin, P. M. Marcum, T. L. Roellig, J. M. De Buizer, Terry L. Herter, R. Güsten et al., "Early science with SOFIA, the stratospheric observatory for infrared astronomy," *The Astrophysical Journal Letters,* vol. 749, no. 2, p. L17, March 2012.
[8] C. Walker, C. Kulesa, P. Bernasconi, H. Eaton, N. Rolander, C. Groppi, J. Kloosterman *et al*., "The Stratospheric THz Observatory (STO)," in *SPIE Astronomical Telescopes+ Instrumentation*, 2010, pp. 77330N-77330N.
[9] A. Young, C. Walker, C. Kulesa, P. Bernasconi, R. Dominguez, J. Siles, et al., "Stratospheric Terahertz Observatory 2016, Sub-orbital flight from

McMurdo, Antarctica," in *Proc. 28th Int. Symp. Space Terahertz Technol.*, 2017.
[10] F. M. Boussaha, J. H. Kawamura, J. A. Stern, A. Skalare and V. White, "A Low Noise 2.7 THz Waveguide-Based Superconducting Mixer," in *IEEE Transactions on Terahertz Science and Technology*, vol. 2, no. 3, pp. 284-289, May 2012.
[11] A. Tang, T. Reck and G. Chattopadhyay, "CMOS system-on-chip techniques in millimeter-wave/THz instruments and communications for planetary exploration," in *IEEE Communications Magazine*, vol. 54, no. 10, pp. 176-182, October 2016.
[12] S. Paine, private communication, 2016.
[13] J. V. Siles, J. Kawamura, R. Lin, C. Lee, and I. Mehdi, "Ultra-Compact THZ Multi-Pixel Local Oscillator Systems for Balloon-borne, Airborne and Space Instruments," in *Proc. 28th Int. Symp. Space Terahertz Technol.*, 2017.
[14] J. Kawamura, J. Kloosterman, J. Siles, F. Boussaha, B. Bumble, V. White, *et al.,* "Development of a 16-pixel monolithic 1.9 THz superconducting waveguide HEB mixer," *Proc. 28th Int. Symp. Space Terahertz Technol.*, 2017.
[15] K. K. Davis, J. Kloosterman, C. Groppi, J. Kawamura, and M. Underhill, "Micro-Machined Integrated Waveguide Transformers in THz Pickett-Potter Feedhorn Blocks," *Proc. 28th Int. Symp. Space Terahertz Technol.*, 2017.
[16] J.V. Siles, I. Mehdi, C. Lee, R. Lin, J.Kawamura, E. Schlecht, *et al.,* "A multi-pixel room-temperature local oscillator subsystem for array receivers at 1.9 THz," in *Proc. of SPIE Astronomical Telescopes+ Instrumentation*, 2014 pp. 914777-914777.